

Performance of Deep Learning in Land Use Land Cover Classification of Indian Remote Sensing (IRS) LISS – III Multispectral Data

Nirav Desai¹, Parag Shukla²

¹Department of computer applications

Atmiya University,

Rajkot, INDIA

niravdesai.research@gmail.com

²Security and digital forensics

NFSU,

Gandhinagar, INDIA

parag.shukla@nfsu.ac.in

Abstract—Identification of land use land cover is a very important task. However, methods existing for the above mention purpose are labor incentives, time-consuming, and costly. Remote sensing plays very important role in the mappings. classification of land cover features and offers very noteworthy and sensed information. The present study shows the semantic segmentation of Indian remote sensing (IRS) LISS-III multispectral image and the comparison of three algorithms U-Net, Deeplabv3+ and Tiramisu. The deep neural network was used to perform the study. We present total 3 innovative datasets, built on these LISS-III images that has 4 different spectral bands (Band – 2 (Blue), Band-3 (Green), Band-4(Red), and Band-5 (Nearly Infrared), FCC (false color composite) images and the ground truth mask images. Dataset has 13500 labelled images. A fully-convolutional network (FCN) with skip connections is trained to take an input image of size 128 X 128 X 3 and outputs a matrix of shape 128 X 128 X 4 i.e., a one-hot encoded version of the mask. The experiment identifies 4 classes successfully (Water Bodies, Vegetation, Uncultivated Land, and Residential areas). The experiment showed that the U-Net algorithm has a very good capability for the classification of LISS -III images for land use land cover class detection then Tiramisu and Deeplabv3+. U-Net achieved accuracy 84%, Deeplabv3+ achieved 29% whereas Tiramisu achieved accuracy 33%.

Keywords- land use land cover, deep learning, FCN, U-Net, Deeplabv3+, Tiramisu

I. INTRODUCTION

In new aeras, satellite images are fetching an immense substance of data for studying the spatial and progressive variability of ecological situations. The beginning of remote sensing with multispectral images in digital format has taken a new dimension in, mapping and monitoring of natural resources of the Earth [9]. Remote sensing is the art of discover and understanding the data or information from a long distance, using sensors without communication with the object being observed [22]. Land use land cover classification anticipates to form space-born images into a precise class, which was reliant on the distribution of predictable land use land cover classes. Land use and land cover mapping are essential errands for preparation and management.

Land use land cover classification using remote sensing images has been applied in several studies, including surveys involving environmental monitoring and change detection [3], research on urbanization effects [24],[10] and disaster mitigation [26]. The spatial resolution of remote-sensing systems is low, so it is probable to recognize the different classes on the Earth's

surface [25]. In 2006, Deep learning projected by Hinton et al. [8] and confirmed training complications of a deep neural network can be solved using one-by-one layer initialization. And efficiently applicable to the field of video and image processing, a field of data analysis [5]. The deep learning algorithms gives a new way for remote sensing image explanation and a massive number of deep learning algorithm research in the field of remote sensing image classification. Semantic Segmentation is defined as a pixel-level classification of images where a class is allotted to an individual pixel of the image.

Remotely sensed imagery is an image data with intervallic Earth observation. The appealing benefits of deep neural networks have been presented in many remote-sensing applications.

Deep neural networks (DNNs) refer to end-to-end mappings (i.e., from data to information) by stacking a large number of filters learned from massive samples. In deep learning, mainly Convolutional Neural Networks (CNNs), have been effectively applied for image classification, target detection, and scene understanding [4][7][12][14][28]. A fully convolutional neural

network (FCN) was proposed by in 2015[17]. FCN is fully related with layers in CNN with up-convolutional layers and concatenates with a shallow, finer layer to produce end-to-end labels. FCN is more fitting for pixel-based image classification, i.e., labelling all pixel to a separate class. The FCN framework has also revealed excessive potential in remote sensing image classification. The U-Net model projected by [21] is an improved FCN model characterized by balanced U-shaped architecture covering a symmetric contracting path and expansive path. Tiramisu is a polyhedral compiler for dense and sparse deep learning and data-parallel algorithms and points a vast set of loop optimizations and data design variations. Deeplabv3+ is a state-of-the-art semantic segmentation model having encoder-decoder architecture.

The present study accomplished the semantic segmentation on datasets (dataset of 13500 images of different seasons) of LISS -III remote sensing images (South Gujarat Region, INDIA). A fully-convolutional network (FCN) with skip connections is trained to take an input image of size 128 x 128 x 3 and outputs a matrix of shape 128 x 128 x 4 i.e., a one-hot encoded version of the mask. In the study 4 classes have been identified - Water Bodies, Vegetation, Uncultivated Land, and Residential areas. U-Net DeepLabv3+ and Tiramisu were applied to perform land use land cover classification on the LISS - III multispectral remote-sensing image. U-Net gives better performance than DeeplabV3+ and Tiramisu. U-Net achieved very good accuracy 84%, Deelabv3+ achieved 29% whereas Tiramisu achieved accuracy 33%.

II. LITERATURE REVIEW

In the deep learning technique numerous layers of data processing phases in ordered architectures are exploited by unsupervised learning and pattern classification [20]. [16] proposed planned and complete assessment of various groups of applying DL methods. [18] proposed DFS algorithm and compare it with YOLOv2. The dataset derives from Google Earth and detects 6 objects airplanes, boats, warehouses, large ships, bridges, and ports. [13] proposed classification technique for land use land cover classification using neural network with random forest. [9] performs pixel and object-based classification and achieves 87% accuracy from satellite images. [23] used Maximum likelihood to perform classification on images of SPOT, ASTER, and Landsat TM for. And achieved OOA of 85.33%, 86.67%, 88.33%, and 86.38% for the years 1989, 2000, 2010, and 2016 respectively. [19] proposed methods that improved convolutional neural networks for aerial image segmentation.[24] proposed object-based Classification for remote sensing image of Deimos-2 and Cartosat-1 using the Convolution Neural Network.

III. USE MATERIALS AND METHODS

In the deep learning technique numerous layers of data processing phases in ordered architectures are exploited by unsupervised learning and pattern classification [20]. [16] proposed planned and complete assessment of various groups of applying DL methods. [18] proposed DFS algorithm and compare it with YOLOv2. The dataset derives from Google Earth and detects 6 objects airplanes, boats, warehouses, large ships, bridges, and ports. [13] proposed classification technique for land use land cover classification using neural network with random forest. [9] performs pixel and object-based classification and achieves 87% accuracy from satellite images. [23] used Maximum likelihood to perform classification on images of SPOT, ASTER, and Landsat TM for. And achieved OOA of 85.33%, 86.67%, 88.33%, and 86.38% for the years 1989, 2000, 2010, and 2016 respectively. [19] proposed methods that improved convolutional neural networks for aerial image segmentation.[24] proposed object-based Classification for remote sensing image of Deimos-2 and Cartosat-1 using the Convolution Neural Network.

A. Data Acquisition

The present study was performed on the South Gujarat Region, State of Gujarat, country INDIA using Indian Remote Sensing (IRS) LISS- III Multispectral remote sensing images. These multispectral images have less than or equal to 10 bands and over 100 nm resolution; have a total of 4 diverse bands in isolated .tiff files and the number of bands is Band – 2,3,4 and 5(Blue, Green, Red, and near Infrared). Quadrats of 30m X 30m size were placed across the study area. Data was acquired from the website of ISRO (<https://bhuvan-app3.nrsc.gov.in>)

A widespread ground study was accomplished to gather environmental landscapes and circulation forms of dissimilar land use and land cover. The GCPs held in reserve for the individual groups were dependent on the distribution of identified land use land cover classes within the study area. The Latitude, Longitude for the location of the respective class is being verified and recorded which are called Ground Control Points (GCPs). GPS device used to collect GCPs. GPS Garmin – eTrex 30 is used for the study. The GCPs reserved for the respective category were reliant on the allocation of recognized land use classes within the study area.

B. Pre-Processing

Indian Remote Sensing (IRS) LISS - III multispectral images have 4 bands. The false color composite (FCC) image was created using combination of these bands. FCCs were designed using stack up these multiband.TIFF image files by the grouping of Band – 4 (Red), Band – 3 (Green), and Band – 2 (Blue). The ground truth masks were designed to train the model after the

creation of FCCs for each image. These Masks were created using the maximum likelihood algorithm on the region of interest for each class.

The study was accomplished on a novel dataset that contains the FCC image of different seasons and the Ground Truth Masks. FCCs and their corresponding masks are resized to 1024 * 1024 pixels then after divided into patches of size 128 x 128 pixels with a striding of 64.

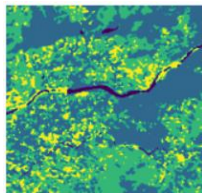


Figure 1. FCC Image

Figure 2. Ground Truth Mask

The size of the dataset was 13500 images where 11250 images are used to train the model while 2250 images are reserved for validation and evaluation.

C. Methods

The maximum likelihood (ML) classifier was used with IRS LISS- III multispectral image data, where every pixel with the maximum likelihood is classified into the matching class. In maximum likelihood, a pixel is selected for a class based on its chance of fitting. Mean vector and covariance metrics are the main necessities of the ML that can be enhanced from training data [23].

Following is a Discriminant Functions Calculated for Each Pixel:

$$g_i(\mathbf{x}) = \ln p(\omega_i) - 1/2 \ln |\Sigma_i| - 1/2(\mathbf{x} - \mathbf{m}_i)^t \Sigma_i^{-1} (\mathbf{x} - \mathbf{m}_i) \quad (1)$$

Where i is class, \mathbf{x} is n -dimensional data in which n represents the total number of bands. $p(\omega_i)$ represents the chance that class ω_i occurs in the image, $|\Sigma_i|$ is the determinant of the covariance matrix, Σ_i^{-1} is an inverse matrix the mean vector represents by \mathbf{m}_i .

Fig.3 shows the basic concepts of maximum likelihood [23]. Ground truth masks were created after the creation of FCC images and used for model training.

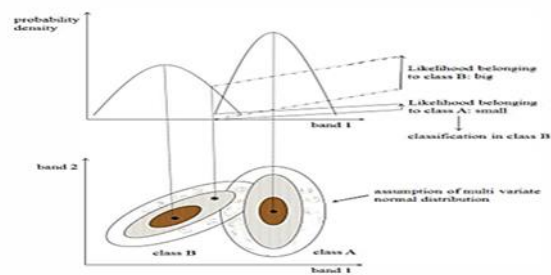


Figure 3: Basic concept of ML [23]

Fully convolutional networks (FCNs) are efficiently applied in the fields like segmentation of an image [1],[9], and medicinal image analysis [6],[15]. FCN is extensively applied in pixel-based classification and used an encoder for feature extraction and a decoder to re-establish the.

A fully-convolutional network (FCN) with skip connections is trained to take an input image of size 128 x 128 x 3 and outputs a matrix of shape 128 x 128 x 4 i.e., a one-hot encoded version of the mask. The FCN is a U-Net architecture that contains an encoder part and a decoder part. The encoder part contains 5 blocks and each block is 2 (convolution + batch normalization + relu) layers stacked on top of one another and trailed by a max-pooling except for the last block. The output of this encoder part is then inputted into the decoder containing 4 blocks. Each block in the decoder starts with an upsampling of the input followed by a 1 x 1 convolution operation. A skip connection is also used that concatenates the output of the corresponding encoder block to the output of the upsampling and convolution operation. The concatenated tensor is then again passed to two convolution layers similar to that of the corresponding encoder block. The output of the decoder part is finally fed to a 1 x 1 convolution with the number of filters equivalent to the number of classes which is 4. Fig. 4 shows the U-Net architecture [17]. The arrows denote the various processes, the black containers denote the feature map and the gray containers denote the cropped feature maps from the contracting path.

$$E = \sum w(x) \log (P_{k(x)}(x)) \quad (2)$$

Where p_k is the pixel-wise SoftMax function applied over the final feature map.

$$P_k(x) = \frac{e^{a_k(x)}}{\sum_{k=1}^K e^{a_k(x)}} \quad (3)$$

And $a_k(x)$ denotes the activation in channel k .

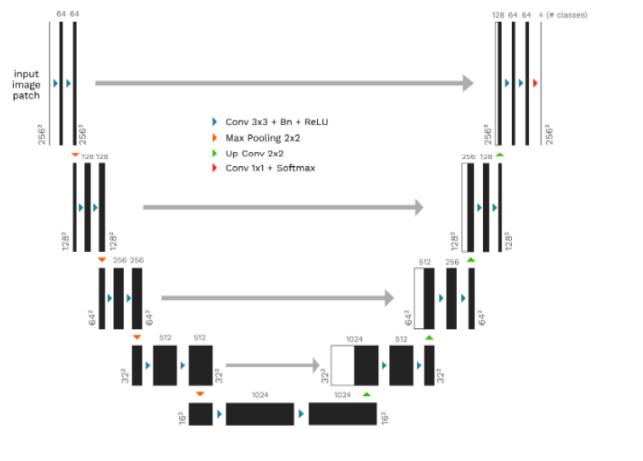


Figure. 4 U-Net architecture

DeepLabv3+ is a state-of-the-art semantic segmentation model having encoder-decoder architecture. The encoder consisting of a pre-trained CNN model is used to get encoded feature maps of the input image, and the decoder reconstructs output from the essential information extracted by the encoder using upsampling. Fig. 5 shows the DeepLabv3+ architecture [2]. DeepLabv3+ extends DeepLabv3 by adding an encoder-decoder structure. The encoder module processes multiscale contextual information by applying dilated convolution at multiple scales, while the decoder module refines the segmentation results of a long object boundary. As go deeper in the network by dilated convolution, can keep the stride constant but with a bigger field-of-view without growing the number of parameters or the amount of calculation. Also, it permits bigger output feature maps, which is useful for semantic segmentation. The purpose of using Dilated Spatial Pyramid Pooling is that it was shown that as the sampling rate becomes bigger, the number of valid filter weights becomes lesser.

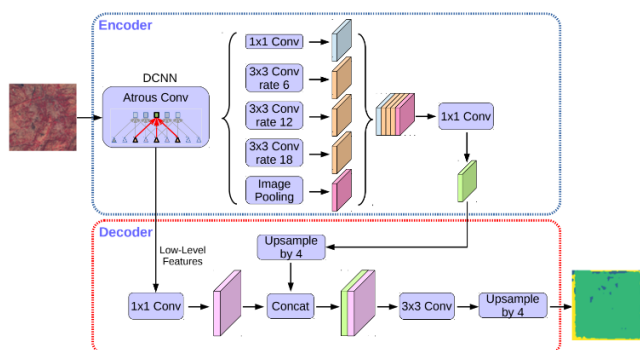


Figure 5: DeepLabv3+

Tiramisu is a polyhedral compiler for dense and sparse deep learning and data-parallel algorithms and directs a huge set of loop optimizations and data design alterations. It is the only open-source DNN compiler that optimizes sparse DNNs and

marks distributed architectures. It can perform complex loop transformations and uses dependence investigation to assure the accuracy of optimizations. Tiramisu has also demonstrated its performance on various standards like deep learning operations (Convolution, ReLu, MaxPool, Sparse Neural Networks, etc.) and linear algebra. However, the Tiramisu network, which itself is a modified U-Net, is much larger and took longer to train. Fig. 6 shows the tiramisu architecture.

$$x_1 = H_1(x_{1-1}) \quad (4)$$

in standard convolution, x_1 is computed by applying a non-linear transformation H_1 to the output of the previous layer x_{1-1} .

$$x_1 = H_1(x_{1-1}) + x_{1-1} \quad (5)$$

ResNet introduces a residual block that sums the identity mapping of the input to the output of a layer

$$x_1 = H_1([x_{1-1}, x_{1-2}, \dots, x_0]) \quad (6)$$

DenseNet input concatenates all previous feature outputs in a feedforward fashion for convolution.

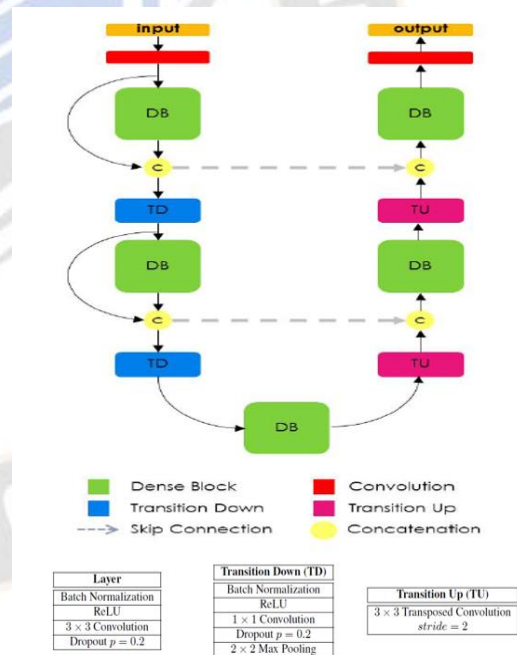


Figure 6. Tiramisu Architecture [29]

D. Training Configuration

While data ingestion, standardize the input images by clipping them to [0.0, 255.0] while the masks are one-hot encoded according to the total number of classes. Random augmentations are applied to the bunch of images and masks before passing them to the model for training. This enlarges the dataset and makes the model robust enough to encounter

dissimilar orientations than just the training data. And it prevents overfitting when augmentations are done correctly. A custom image data generator is created to fulfill the requirements of this data ingestion pipeline. Table No.1 represents the hyperparameters and other configurations for model training.

TABLE . 1 HYPERPARAMETERS AND OTHER CONFIGURATIONS USED FOR TRAINING THE MODEL.

Hyperparameters & Configurations	Values
Train Batch Size	16
Validation Batch Size	16
Input Image Shape	128,128,3
Number of classes	4
Epochs	50
Loss	Categorical Focal Loss*
Optimizer	Adam
Metrics	Dice Coefficient*
Class Weights	[1.69941, 0.53043, 1.23977, 1.38949]

IV. RESULT

The algorithm for classification developed in U-Net, Deeplabv3+ and Tiramisu was coded with python + OpenCV. The experiment performed the best fine-tuning parameters for U-net, Deeplabv3+ and Tiramisu with RGB bands of the dataset of IRS LISS- III multispectral remote sensing images. The

parameters which give very good performance are used to develop the final model. The model also used data augmentation.

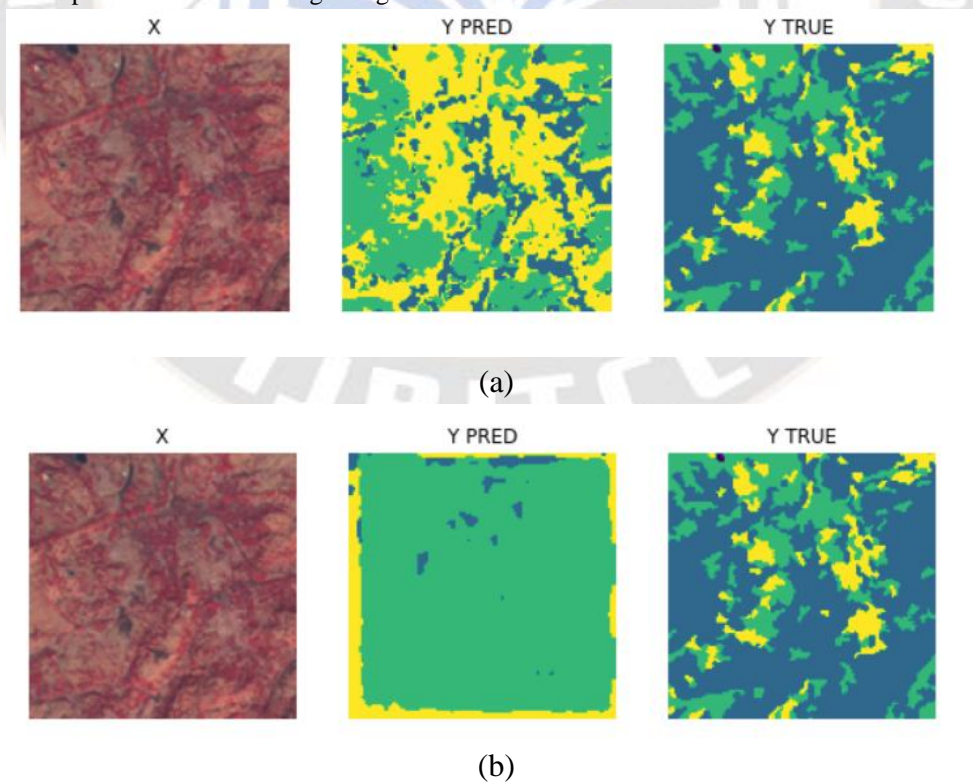
TABLE 2 EXPERIMENT RESULT

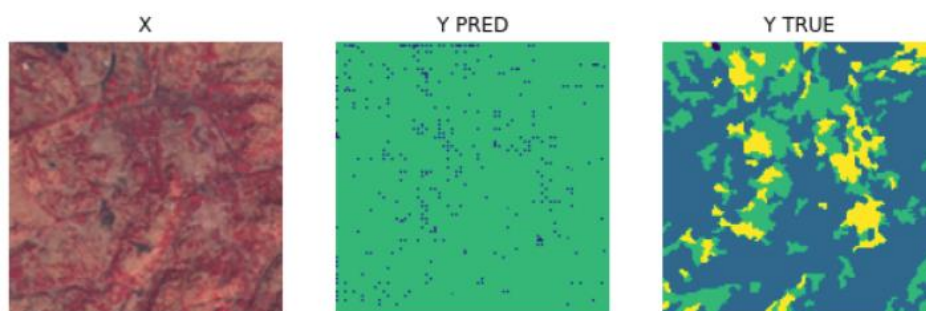
Sr.No	Algorithm	Optimizer	EPOCH Trained	Accuracy
a	U-Net	Adam	50	84
b	Deeplabv3+	Adam	50	29
c	Tiramisu	Adam	50	33

Table -2 shows the experiment results and accuracy with different epochs. And from the outcomes, it was noticed that U-net gives healthier results in classifying land use land cover classes. Fig. 7 shows the predicted results.

Fig. 7 shows the land use land cover classification by the U-Net model. Fig.7(b) show the classification of land use land cover by Deeplabv3+ and Fig. 7(c) shows the result predicted by the model Tiramisu. Water Bodies are black, Vegetation is light green, Uncultivated Land is light blue, and Residential Areas in yellow.

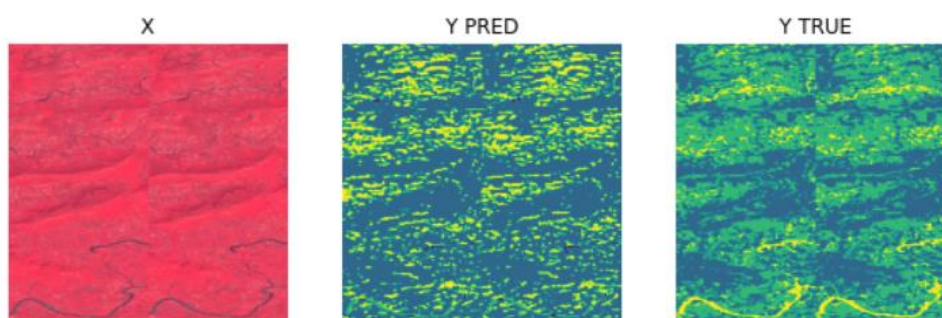
Fig. 8 shows the quantification for each respective class after classification was performed. The values 0 – represent water, 1 represents vegetation, 2 represents uncultivated land and 3 represents the residential area.





(c)

Figure. 7 Result



```
{0: 1.2038230895996094}
{0: 1.2038230895996094, 1: 83.2174301147461}
{0: 1.2038230895996094, 1: 83.2174301147461, 2: 3.7054061889648438}
{0: 1.2038230895996094, 1: 83.2174301147461, 2: 3.7054061889648438, 3: 11.873340606689453}
```

Figure. 8 Quantification

V. CONCLUSION

The proposed model achieved very good accuracy in the land use land cover classification using a deep learning approach. Deep learning for LULC classification becoming more evident. It will deliver a cost-effective and time management resolution than the visual understanding. The grouping of maximum Likelihood for ground truth masking and U-net for classification gives better results. In the present study, we proposed a land use land cover classification model built on U-Net, Deeplabv3+ and tiramisu algorithms. The models were trained and tested on LISS-III multispectral space-borne image dataset. Experiments show that model detected a total of 4 land use land cover classes i.e., Water body, vegetation, uncultivated land, and residential with very good accuracy. Results predicted by the model confirmed that the U-Net classifier holds gigantic potential for accurate detection of land use land cover classes than deeplabv3+ and tiramisu. The U-Net model achieves a very good accuracy of 84 %.

REFERENCES

- [1] Bi, L., Kim, J., Ahn, E., Kumar, A., Feng, D., & Fulham, M. (2019). Step-wise integration of deep class-specific learning for dermoscopic image segmentation. *Pattern recognition*, 85, 78-89.
- [2] Chen, L. C., Papandreou, G., Kokkinos, I., Murphy, K., & Yuille, A. L. (2017). Deeplab: Semantic image segmentation with deep convolutional nets, atrous convolution, and fully connected crfs. *IEEE transactions on pattern analysis and machine intelligence*, 40(4), 834-848.
- [3] Chen, Y.-C., Chiu, H.-W., Su, Y.-F., Wu, Y.-C., and Cheng, K.-S. (2017). Does urbanization increase diurnal land surface temperature variation? Evidence and implications. *Landscape Urban Plann.* 157, 247–258. doi:10.1016/j.landurbplan.2016.06.014
- [4] Codts, M.; Omran, M.; Ramos, S.; Rehfeld, T.; Enzweiler, M.; Benenson, R.; Franke, W.; Roth, S.; Schiele, B. The cityscapes dataset for semantic urban scene understanding. In *Proceedings of the IEEE conference on computer vision and pattern recognition (CVPR)*, Las Vegas, NV, USA, 27–30 June 2016; pp. 3213–3223.
- [5] Dian-lai, W., Ai-xia, S., & Wen-ping, L. (2020, November). Application of deep neural networks in classification of

- medium resolution remote sensing image. In *Journal of Physics: Conference Series* (Vol. 1682, No. 1, p. 012014). IOP Publishing.
- [6] Fan, J., Cao, X., Yap, P. T., & Shen, D. (2019). BIRNet: Brain image registration using dual-supervised fully convolutional networks. *Medical image analysis*, 54, 193-206.
- [7] Fu, G.; Zhao, H.; Li, C.; Shi, L. Segmentation for High-Resolution Optical Remote Sensing Imagery Using Improved Quadtree and Region Adjacency Graph Technique. *Remote Sens.* 2013, 5, 3259–3279.
- [8] Hinton, G. E., Osindero, S., & Teh, Y. W. (2006). A fast learning algorithm for deep belief nets. *Neural computation*, 18(7), 1527-1554.
- [9] Huang, Y., Zhou, F., & Gilles, J. (2019). Empirical curvelet based fully convolutional network for supervised texture image segmentation. *Neurocomputing*, 349, 31-43.
- [10] Hung, W.-C., Chen, Y.-C., and Cheng, K.-S. (2010). Comparing landcover patterns in Tokyo, Kyoto, and Taipei using ALOS multispectral images. *Landscape Urban Plann.* 97, 132–145. doi:10.1016/j.landurbplan.2010.05.004
- [11] Karoui, M. S., Deville, Y., Hosseini, S., Ouamri, A., & Ducrot, D. (2009, August). Improvement of remote sensing multispectral image classification by using independent component analysis. In *2009 First Workshop on Hyperspectral Image and Signal Processing: Evolution in Remote Sensing* (pp. 1-4). IEEE.
- [12] Krizhevsky, A.; Sutskever, I.; Hinton, G.E. ImageNet classification with deep convolutional neural networks. In *Proceedings of the Neural Information Processing Systems (NIPS) Conference, La Jolla, CA, USA, 3–8 December 2012*.
- [13] Lateef, F., & Ruichek, Y. (2019). Survey on semantic segmentation using deep learning techniques. *Neurocomputing*, 338, 321-348.
- [14] Lecun, Y.; Bengio, Y.; Hinton, G. Deep learning. *Nature* 2015, 521, 436–444.
- [15] Li, C., Wang, X., Liu, W., Latecki, L. J., Wang, B., & Huang, J. (2019). Weakly supervised mitosis detection in breast histopathology images using concentric loss. *Medical image analysis*, 53, 165-178.
- [16] Li, L., Han, L., Ding, M., Cao, H., & Hu, H. (2021). A deep learning semantic template matching framework for remote sensing image registration. *ISPRS Journal of Photogrammetry and Remote Sensing*, 181, 205-217.
- [17] Long, J.; Shelhamer, E.; Darrell, T. Fully convolutional networks for semantic segmentation. In *Proceedings of the IEEE Conference on Computer Vision and Pattern Recognition (CVPR), Boston, MA, USA, 5–7 June 2015*; pp. 3431–3440
- [18] Minaee, S., Boykov, Y. Y., Porikli, F., Plaza, A. J., Kehtarnavaz, N., & Terzopoulos, D. (2021). Image segmentation using deep learning: A survey. *IEEE transactions on pattern analysis and machine intelligence*.
- [19] Moreira, R. C. (2008). Estudo espectral de alvos urbanos com imagens do sensor HSS (Hyperspectral Scanner System) (Doctoral dissertation, PhD Thesis, National Institute for Space Research (INPE)).
- [20] Mohanty, S. P., Czakon, J., Kaczmarek, K. A., Pyskir, A., Tarasiewicz, P., Kunwar, S., ... & Schilling, M. (2020). Deep learning for understanding satellite imagery: An experimental survey. *Frontiers in Artificial Intelligence*, 3, 534696.
- [21] Ronneberger, O., Fischer, P., & Brox, T. (2015, October). U-net: Convolutional networks for biomedical image segmentation. In *International Conference on Medical image computing and computer-assisted intervention* (pp. 234-241). Springer, Cham.
- [22] Sarah C. Goslee" Analyzing Remote Sensing Data in R: The Landsat Package", *Journal of Statistical Software*, July 20i I, Volume 43, Issue <http://www.jstatsoft.org>
- [23] Schowengerdt, R. A. (2006). *Remote sensing: models and methods for image processing*. Elsevier.
- [24] Suneetha, Manne, et al. "Object based Classification of Multispectral Remote Sensing Images for Forestry Applications." *Proceedings of the 2020 3rd International Conference on Image and Graphics Processing*. 2020.
- [25] Teng, S. P., Chen, Y. K., Cheng, K. S., and Lo, H. C. (2008). Hypothesis-test-based landcover change detection using multi-temporal satellite images – A comparative study. *Adv. Space Res.* 41, 1744–1754. doi:10.1016/j.asr.2007.06.064
- [26] Xu, X., Chen, Y., Zhang, J., Chen, Y., Anandhan, P., & Manickam, A. (2021). A novel approach for scene classification from remote sensing images using deep learning methods. *European Journal of Remote Sensing*, 54(sup2), 383-395.
- [27] Yang, C., Luo, J., Hu, C., Tian, L., Li, J., and Wang, K. (2018). An observation task chain representation model for disaster process-oriented remote sensing satellite sensor planning: a flood water monitoring application. *Remote Sens.* 10, 375. doi:10.3390/rs10030375
- [28] Zhang, L.; Zhang, L.; Du, B. Deep learning for remote sensing data: A technical tutorial on the state of the art. *IEEE Geosci. Remote Sens. Mag.* 2016, 4, 22–40.
- [29] <https://towardsdatascience.com/review-fc-densenet-one-hundred-layer-tiramisu-semantic-segmentation-22ee3be434d5>